ELSEVIER

Ceramics International 32 (2006) 441–446

CERAMICS INTERNATIONAL

www.elsevier.com/locate/ceramint

Crystallization kinetics of plasma sprayed basalt coatings

Gunhan Bayrak, Senol Yilmaz *

Sakarya University, Engineering Faculty, Department of Metallurgical and Material Engineering, Esentepe Campus, 54187 Sakarya, Turkey

Received 5 January 2005; received in revised form 14 February 2005; accepted 15 March 2005
Available online 31 August 2005

Abstract

Crystallization kinetics concerning the conversion of a glass coating layer made from natural basalt volcanic rock to glass-ceramic have been investigated. The basalt-based coatings were deposited on AISI 1040 steel substrates pre-coated with Ni–5 wt.% Al using atmospheric plasma spraying system. Glass coatings were heat treated at 800, 900 and 1000 °C for 1–4 h in order to obtain glass-ceramic coating layer. DSC and XRD analysis revealed the crystallization of augite [$(CaFeMg)SiO_3$]. Heat treatment is effective for the amorphous phase to convert into crystalline in atmospheric plasma sprayed basalt coating depending on heat treatment time and temperature. Optical microscopy was used for metallographic examinations. The kinetics of the augite was studied by applying DSC measurements carried out different heating rates and the activation energies of crystallization and viscous flow were measured as 324 and 364 kJ mol^{-1}, respectively. Avrami exponents for crystallization were 1.85–2.74 which indicates that internal crystallization dominates the overall crystallization.

Keywords: D. Glass-ceramic; Basalt; Plasma spray coating; Crystallization; Kinetics

1. Introduction

Plasma spraying has become a widely accepted method for producing ceramic coatings that are used to protect metallic structural components from corrosion, wear, and erosion, and to provide lubrication and thermal insulation [1–3]. The plasma spraying involves injection of particles into a plasma jet of temperature up to 15 000 K and velocity up to 1 km s^{-1}. The objective is to just melt the powder completely and accelerate it to maximum velocity towards the target [4,5]. In the plasma spraying technique, coating layers are formed by the building-up of melted or partially melted droplets that flatten after collision onto a substrate by mechanical bonding to surface imperfections [6,7]. Nearly any material that can be produced in powder form can be deposited by plasma spraying. The characteristics of the precursor powder that influence the plasma coating microstructure have been identified as size distribution, flow ability, morphology, density and chemical composition, which depend on their means of production [7]. Plasma spray techniques are suitable for glassy coatings because of their high temperature process conditions [8,9].

Basalt is a grey to black, fine-grained volcanic rock. Basalt forms a black homogenous glass when cooled from the molten stage and subsequent reheating above annealing temperature results in the development of fine-grained glass-ceramics [10]. Superior abrasion, wear and chemical resistant basalt-based glass-ceramics can be produced from the basalt. They can be used wherever the transport of material causes mechanical or chemical abrasion as well as mineral wool for heat, noise and fire insulation [10–13].

Although many investigations have been performed on development of plasma spray coatings, not much effort has been made to use natural raw materials such as basalt for plasma spray purposes. When the natural volcanic basalt rocks ground into powder form, it can be used as a plasma spray coating powder. Glassy basalt coatings in amorphous phase can be transformed to glass-ceramic form with suitable heat treatment. The aim of this paper is to examine details of the crystallization kinetics of basalt-based coatings and clarify some typical aspects of the crystallisation.

* Corresponding author. Tel.: +90 264 346 03 53/402; fax: +90 264 346 03 51.
E-mail address: symaz@sakarya.edu.tr (S. Yilmaz).

0272-8842/$30.00
doi:10.1016/j.ceramint.2005.03.032

2. Experimental procedure

Natural basalt volcanic rocks obtained from the Middle Anatolia region of Turkey were used in coatings. Basalt rocks were obtained as a chunk and crashing was carried out in a jaw and conic crushers. The resultant powder was then ground using ring grinder and sieved to the particle size of $-53 + 45$ μm for coating. The chemical composition of volcanic basalt rock analyzed quantitatively using Perkin-Elmer 2300 atomic absorption spectroscopy is given in Table 1. The substrate used in this study was AISI 1040 steel, chemical analysis of which was determined using Thermo Jarrel ASH-BAIRD Corp. DV-6S 3063A model spectral analyzer, with the dimensions of 20 mm in diameter and 5 mm in height. Chemical analysis of steel substrate that prepared metallographically by polishing with 1000 grid emery paper in the final stage is reported in Table 2. The surface of substrates was grit-blasted with 35 grid alumina under conditions 2 bar pressure, an angle of 45°, a spray distance of 50 mm and a flow rate of 2 kg min^{-1} and followed by ultrasonic cleaning in an ethyl alcohol and acetone solvent for 15 min and dried. Basalt powders were sprayed on substrates with a Ni–5 wt.% Al bond coat by plasma spray technique with a hand-controlled plasma spray system. The plasma spray parameters are given in Table 3.

To remove thermal residual stress, all coated samples were immediately annealed in a furnace at 600 °C for 1 h followed by slow cooling to room temperature. The annealed coatings were found to be amorphous by X-ray diffraction analysis (XRD). Glass-ceramic coated samples were prepared by applying suitable heat treatments planned according to the differential scanning calorimeter (DSC) results of the amorphous coatings. Heat treatments were carried out at temperatures of 800, 900 and 1000 °C in the argon atmosphere by a Lenton tube furnace with a time ranging from 1 to 4 h to promote internal crystallization. The crystallization temperatures were selected from the DSC curve depending on the endothermic and exothermic reaction temperatures. XRD technique with a Cu Kα wavelength of 1.5418 Å was used to analyze the crystalline structure and phases present in the coatings before and after heat treatment. Some of the crystallized specimens were mounted in conductive resin, grinded with SiC paper and finally polished with a 1 μm diamond slurry to observe morphological details using BHM 313 U Olympus optical microscope. An optical micrometer attached to the optical microscope measured the thickness of the coating layers deposited on the steel sample.

Table 1
Chemical composition of volcanic basalt rock (Fe_2O_3 represents the total amount of FeO + Fe_2O_3)

Compounds	wt.%
SiO_2	45.88
Al_2O_3	18.20
Fe_2O_3	9.95
CaO	9.28
MgO	6.62
K_2O	1.64
Na_2O	4.76
P_2O_5	1.04
LOI	2.63

Table 2
Chemical composition of AISI 1040 steel substrate

Element	wt.%
C	0.41
Si	0.20
Mn	0.74
P	0.024
S	0.032
Cr	0.028
Mo	0.019
Ni	0.021
V	0.001

Differential thermal analysis (DTA) and DSC are widely used in investigating the crystallization kinetics of glasses and glass-ceramics. In this study, the crystallization kinetics of basalt coatings were studied by DSC to determine the peak temperatures (glass transition and crystallization) and for calculating activation energies for the crystallization and the viscous flow. After crushing, pulverising and grinding of coatings on the steel substrate to a powder size of about 30 μm, DSC experiment were performed by TA instrument 2010 thermoanalyser with heating rates of 5, 10 and 15 °C min^{-1}. All DSC experiments were carried out in air atmosphere up to 1100 °C temperature.

3. Results and discussion

3.1. Microstructure and crystalline phases

Fig. 1 shows the optical microstructure of basalt coated AISI 1040 steel sample including three distinct regions which are: (i) the main basalt coating layer, (ii) the bond coat between the basalt layer and substrate, and (iii) steel matrix. In this study, a uniform coating including some porosities was obtained (Fig. 1). The thickness of bond coat and basalt-based glass coating layer was measured by optical micrometer as 40 ± 8 and 190 ± 5 μm, respectively.

Table 3
Plasma spray coating parameters

Coating parameter	Value
Plasma gun (MB)	3
Current (A)	500
Voltage (V)	64–70
Gas flow for Ar (l/min)	50
Gas flow for H (l/min)	15
Spray distance (mm)	130
Powder feed rate (g/min)	39
Carrier gas flow (1/min)	3–6

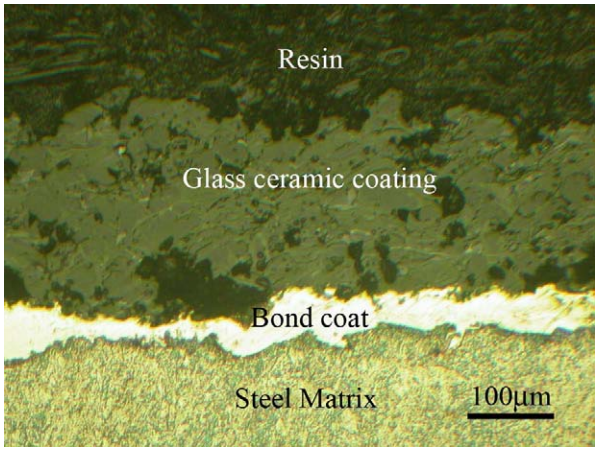

Fig. 1. Optical microstructure of the coating layer.

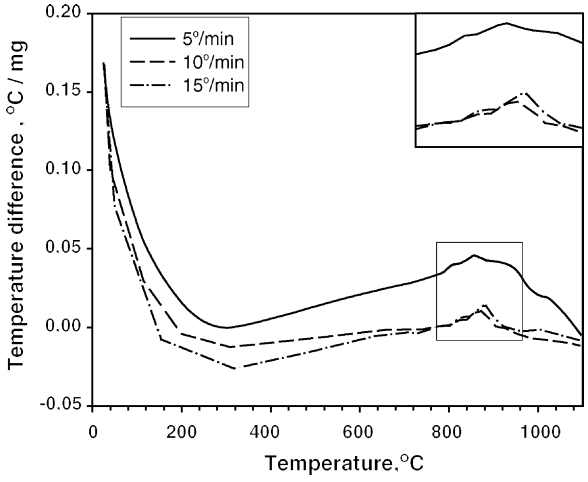

Fig. 3. DSC curves of plasma spray coated basalt-based glasses.

The basalt coating on the steel substrates with Ni–5 wt.% Al interlayer bond coat steel was analyzed by XRD analyses. Fig. 2 shows that XRD patterns of as-sprayed and heat treated coatings at 800, 900 and 1000 °C for 2 h. The as-sprayed coating was found to be amorphous. Plasma spray coating technique can be used for glass coating from the crystalline oxide based ceramics which are suitable for glass formation [8,9]. As it is known, amorphous glass structure is necessary for glass-ceramic production prior to the crystallization heat treatment [11,14]. DSC studies were performed on the glassy coatings to determine the crystallization temperature by different heating rates. DSC curves of coated basalt glass show a small endothermic dip (the glass transition temperature, T_g) and two exothermic peaks indicating the crystallization (Fig. 3) whatever the heating rate. The appearance of two crystallization peaks on the DSC curve implies that at least two different crystal phases are formed during the heat treatment. This was also confirmed by XRD results (Fig. 2). This agrees with previous studies [11,12].

The main crystalline phases formed in the coating were found to be augite [$(CaFeMg)SiO_3$], diopside [$Ca(Mg_{0.15}Fe_{0.85})(SiO_3)_2$] and aluminian-diopside [Ca(Mg, Al)(Si, Al)$_2O_6$] phases confirmed by XRD. These phases are usually referred as one phase named diopsidic-augite in the literature as reported in the studies of Beall and Rittler [10], Yilmaz [11] and Yilmaz et al. [12]. The diopsidic-augite provides superior abrasion and chemical resistance to the basalt-based glass-ceramics [10,13]. It is common to use nucleation agents such as TiO_2, ZrO_2, P_2O_5, etc. in glass-ceramics, especially from pure oxides. However, in basalt glass-ceramics, such nucleation agents are not needed because of the presence of FeO and Fe_2O_3 oxides. It was reported that FeO and Fe_2O_3 in the basalt oxidize to Fe_3O_4, which acts as a nucleation agent and crystal growth site [12,13]. When the crystallization temperature increases, the peak intensity of crystalline phases increases as reported in the literature [11,15,16]. This indicates that increasing the heat treatment temperature causes to the higher crystalline phases in the basalt-based coated glass.

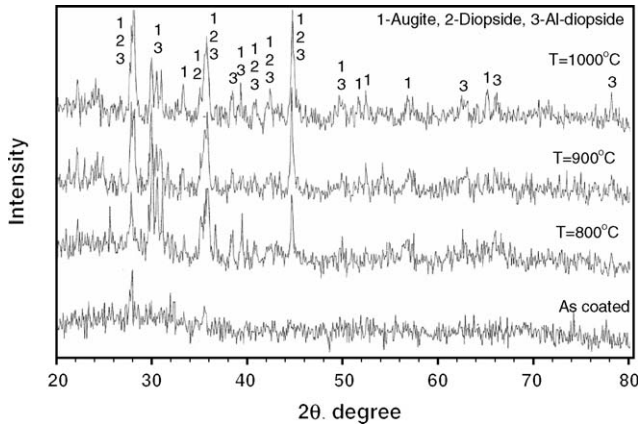

Fig. 2. X-ray diffraction patterns of basalt-based glass-ceramic coatings depending on crystallization temperature for 2 h.

3.2. The kinetics of crystallization

The kinetics for isothermal solid-state phase transformation (here glass to crystal) can be described by the phenomenological Johnson–Mehl–Avrami (JMA) equation [12].

$$X = 1 - \exp[-(kt)^n] \quad (1)$$

Taking natural logarithms and rearranging Eq. (1)

$$\ln[-\ln(1 - X)] = n \ln k + n \ln t \quad (2)$$

can be obtained, where X is the volume fraction crystallized after time t, n is the Avrami parameter which depends on the growth direction number and the mechanism of nucleation and crystal growth shown in Table 4, and k is the reaction rate constant (s^{-1}) which depends on both the nucleation rate and the growth rate [12,17,18]. k may be expected to exhibit

Table 4
Values of parameter n for various crystallization mechanisms [12,13]

Mechanism	n
Bulk nucleation	
Three-dimensional growth	4
Two-dimensional growth	3
One-dimensional growth	2
Surface nucleation	1

an Arrhenius temperature dependence:

$$k = V \exp\left(\frac{-E_a}{RT}\right) \tag{3}$$

or taking natural logarithms

$$\ln k = \ln V - \frac{E_a}{RT} \tag{4}$$

where V is a frequency factor (s^{-1}); E_a, the activation energy for crystallization (J mol^{-1}); R, the gas constant (8.314 J mol^{-1}) and T, the absolute temperature (K) [12].

From the value of the activation energy (E_a), the Avrami parameter (n) can be calculated using the equation presented by Augis and Bennett for non-isothermal analysis as follows;

$$n = \left(\frac{2.5}{\Delta T}\right)\left(\frac{T_p^2}{E_a/R}\right) \tag{5}$$

where ΔT is the full width of the exothermic peak at the half maximum intensity and T_p is crystallization peak temperature [12,17–20]. Consequently, a sharp peak (small ΔT, large n) implies bulk crystallization, while a broad peak (large ΔT, small n) signifies surface crystallization. When the sample is heated at a constant heating rate (β), the temperature (T) of the sample at any time (t) is given by $T = T_i + \beta t$, T_i being the initial starting temperature. The reaction rate constant (k) in Eq. (4), therefore, is no longer a constant but is a function of time, and the transformation mechanism cannot be described by the simple JMA equation (Eq. (2)). A modified form of the JMA equation which takes into account the dependence of k on t is used for non-isothermal crystallization [20]. The value of the activation energy for crystallization of amorphous glassy layer was determined using a modified form of the JMA equation. It was originally applied to crystallization studies by Kissinger and modified by others [12,18–21]. This method is based on the dependence of the

Table 5
DSC measurements of plasma spray coated basalt-based glass

Heating rate, β (K min^{-1})	Peak temperature		ΔT (K)
	T_g	T_p	
5	1060	1129	44
10	1076	1140	34
15	1078	1153	31

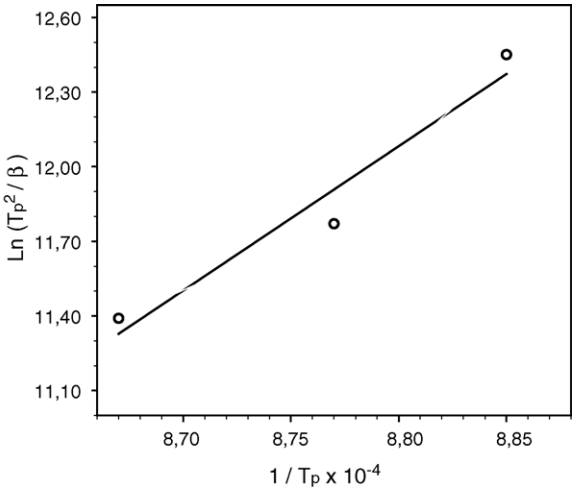

Fig. 4. Plot of $\ln T_p^2/\beta$ vs. $1/T_p$ for the determination of the activation energy for the crystallization of plasma spray coated basalt-based glass.

crystallization peak temperature (T_p) on the DTA or DSC heating rate (β) as follows:

$$\frac{\ln T_p^2}{\beta} = \frac{\ln E_a}{R} - \ln V_a + \frac{E_a}{RT_p} \tag{6}$$

Likewise, Eq. (6) can also be used to predict the viscous energy, as described by Mahadevan et al. [12]:

$$\frac{\ln T_g^2}{\beta} = \frac{\ln E_c}{R} - \ln V_c + \frac{E_c}{RT_g} \tag{7}$$

Here, E_c is the corresponding activation energy for viscous flow, T_g is the glass transformation temperature, V_a is the frequency factor for crystallization and V_c is the frequency factor for viscous flow.

Plots of $\ln T_p^2/\beta$ versus $1/T_p$ and $\ln T_g^2/\beta$ versus $1/T_g$ obtained at various heating rates should be linear with slopes

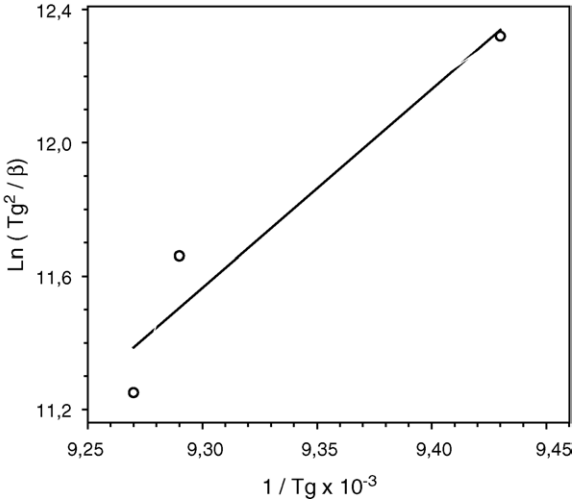

Fig. 5. Plot of $\ln T_g^2/\beta$ vs. $1/T_g$ for the determination of the activation energy for the viscous flow of plasma spray coated basalt-based glass.

Table 6
n-Values of plasma spray coated basalt-based glass

Heating rate, β (K min^{-1})	n	Mechanism
5	1.85	Bulk nucleation, one-dimensional growth
10	2.45	Bulk nucleation, two-dimensional growth
15	2.74	Bulk nucleation, two-dimensional growth

Ea/R and the intercept $[\ln(E_a/R) - \ln V_a]$ and $[\ln(E_c/R - \ln V_c]$. Therefore, if E_a/R and E_c/R are estimated from the slope, the frequency factors can be calculated from the intercept [12]. The peak temperatures (T_g and T_p) changing with heating rates and T values for calculating n are listed in Table 5. The same data are graphically plotted in Figs. 4 and 5.

In accordance with published data, the temperature of the crystallization peak is higher at faster heating rates [12]. The values of E_a, E_c and V_a, V_c obtained from the slope and the intercept of lines (Figs. 4 and 5) were

$$E_a = 324\,\text{kJ mol}^{-1}; \qquad E_c = 364\,\text{kJ mol}^{-1};$$
$$V_a = 3.56 \times 10^{10}\,\text{s}^{-1}; \qquad V_c = 4.01 \times 10^{10}\,\text{s}^{-1}$$

The value of E_a is not in good agreement with the value reported by Voldan et. al. ($E_a = 245$ kJ mol^{-1}) and Yilmaz et al. ($E_a = 238$ kJ mol^{-1}) who studied the kinetics of crystallization of basalt glass using the isothermal method [11–13]. This may be due to difficult crystallization behaviors of the amorphous glassy basalt-based coatings according to melted basalt glass.

The n-values, which were calculated using Eq. (5), are given in Table 6. It can be seen that $n = 1.85$–2.74 which indicates that the crystallization of the amorphous glassy basalt-based coatings at all heating rates is caused by bulk nucleation with one and two-dimensional crystal growth.

4. Conclusion

In the crystallization of the amorphous glassy basalt-based coatings, augite [$(CaFeMg)SiO_3$], diopside [$Ca(Mg_{0.15}Fe_{0.85})(SiO_3)_2$] and aluminian-diopside [Ca(Mg, Al)(Si, Al)$_2O_6$] phases were determined by XRD. These phases are also referred to as one phase named diopsidic-augite. Johnson–Mehl–Avrami, Kissenger, Mahadevan, Augis and Bennett equations were used for the calculation of the activation energies for the crystallization and viscous flow and Avrami parameter. Avrami parameter (n) related to the reaction mechanism was determined by using ΔT values obtained from DSC measurements at different heating rates. Depending on the heating rate, the n-values were found to vary between 1.85 and 2.74, which indicates the bulk nucleation in the amorphous glassy basalt-based coatings by one and two-dimensional crystal growth. The activation energies of the crystallization and viscous flow were calculated as 324 and 364 kJ mol^{-1}, respectively.

Acknowledgements

The authors would like to express their gratitude to Sakarya University Engineering Faculty, and Prof. C. Bindal, the head of the Department of Metallurgy and Material Engineering for supporting this work. The authors express theirs grateful thanks to Technician Ersan Demir and Ebubekir Cebeci at Plasma Spray laboratory of Sakarya University, Turkey, for assisting with experimental studies. The authors are also grateful to Dr. Ugur Sen and Müberra Yılmaz (M.Sc.) for assisting with writing, checking and experimental assistance.

References

[1] P. Bansal, N.P. Padture, A. Vasiliev, Improved interfacial mechanical properties of Al_2O_3–13 wt.% TiO_2 plasma-sprayed coatings derived from nanocrystalline powders, Acta Mater. 51 (2003) 2959–2970.
[2] S. Yilmaz, S.C. Okumus, A.S. Demirkiran, C. Bindal, Fly ash plasma spray coatings, Key Eng. Mater. 264–268 (1–3) (2004) 533–536.
[3] S. Yılmaz, M. Ipek, G. Celebi, C. Bindal, The effect of bond coat mechanical properties of plasma sprayed Al_2O_3 and Al_2O_3–13wt.% TiO_2 coatings on AISI 316L stainless steel, Vacuum 77 (2005) 315–321.
[4] H.M. Hawthorne, L.C. Erickson, D. Ross, H. Tai, T. Troczynski, The microstructural dependence of wear and indentation behaviour of some plasma-sprayed alumina coatings, Wear 203–204 (1997) 709–714.
[5] O. Sarıkaya, Effect of substarate temperature on properties of plasma sprayed Al_2O_3 coatings, Mater. Des. 26 (1) (2005) 53–57.
[6] E. Fleury, S.M. Lee, W.T. Kim, D.H. Kim, Effects of air plasma spraying parameters on the Al–Cu–Fe quasicrystalline coating layer, J. Non-Cryst. Solids 278 (2000) 194–204.
[7] G. Bertrand, C. Filiatre, H. Mahdjoup, A. Foissy, C. Coddet, Influence of slurry characteristic on the morphology of spray-dried alumina powders, J. Eur. Ceram. Soc. 23 (2003) 263–271.
[8] D.T. Weaver, D.C. Vanaken, J.D. Smith, The role of bulk nucleation in the formation of crystalline cordierite coatings produced by air plasma spraying, Mater. Sci. Eng. A 39 (2003) 96–102.
[9] J.A. Helsen, J. Proost, J. Schrooten, G. Timmermans, E. Brauns, Glasses and bioglass: synthesis and coatings, J. Eur. Ceram. Soc. 17 (1997) 147–152.
[10] G.H. Beall, H.L. Rittler, Basalt glass ceramics, Am. Ceram. Soc. Bull. 55 (1976) 579–582.
[11] S. Yilmaz, The Investigation of Production Conditions and Properties of Basalt Glass Ceramics Materials From the Volcanic Basalt Rocks, Ph.D. Thesis, Istanbul Technical University, Istanbul, 1997.
[12] S. Yilmaz, O.T. Ozkan, V. Gunay, Crystallization kinetics of basalt glass, Ceram. Int. 22 (1996) 477–481.
[13] V. Znidarsic, D. Kolar, The crystallization of diabase glass, J. Mater. Sci. 26 (1991) 2490–2494.
[14] P.W. McMillan, Glass-ceramics, second ed., Academic Press, London, 1979.
[15] J.R. Jurado-Egea, A.E. Owen, A.K. Bandyopadhyay, Electronic conduction in basalt glass and glass-ceramics correlation with magnetite crystallization, J. Mater. Sci. 22 (1987) 3602–3606.
[16] A.K. Bandyopadhyay, P. Labarbe, J. Zarzycki, A.F. Wright, Nucleation, Crystallization studies of basalt glass-ceramic by small angle neutron scattering, J. Mater. Sci. 18 (1983) 709–716.
[17] D.C. Clupper, L.L. Hench, Crystallization kinetics of tape cast bioactive glass 45S5, J. Non-Cryst. Solids 318 (2003) 43–48.
[18] A. Karamanov, M. Pelino, Crystallization phenomena in iron-rich glass, J. Non-Cryst. Solids 281 (2001) 139–151.

[19] Y.J. Park, J. Heo, Nucleation and crystallization kinetics of glass derived from incinerator fly ash waste, Ceram. Int. 28 (2002) 669–673.
[20] C.S. Ray, W. Huang, D.E. Day, Crystallization kinetics of a lithia-silica glass: effect of sample characteristics and thermal analysis measurement techniques, J. Am. Ceram. Soc. 74 (1991) 60–66.
[21] M. Erol, S. Kucukbayrak, A.E. Mericboyu, M.L. Ovecoglu, Crystallization behaviour of glasses produced from fly ash, J. Eur. Ceram. Soc. 21 (2001) 2835–2841.